24th INTERNATIONAL CONGRESS ON SOUND AND VIBRATION
23–27 July 2017, London

ICSV24
23-27JULY 2017
LONDON CALLING

NOISE CONTROL FOR A TANDEM AIRFOIL CONFIGURATION USING TRAILING EDGE SERRATION

Xiao Liu, Syamir Alihan Showkat Ali and Mahdi Azarpeyvand
Faculty of Engineering, University of Bristol, Bristol, U.K.
email: xiao.liu@bristol.ac.uk

This paper reports an experimental investigation on the application of serrations as a passive control method for reducing the aerodynamic sound from airfoils in tandem. The aim of the study is to investigate the efficiency of serrated trailing edge on cambered NACA 65-710 tandem airfoil to control and regularize the turbulence flow within the gap between the two airfoils. The wake flow characteristics for a cambered NACA 65-710 airfoil with and without the serration treatment have been quantified using two-dimensional Particle Image Velocimetry (PIV). The surface pressure coefficient distributions and surface pressure fluctuations have been measured using the pressure taps and the remote sensing probe techniques. The results show that the use of serrations at relatively high angles of attack (10 and 15 degree), can lead to a significant reduction of turbulent kinetic energy, which is believed to be due to the interaction between the flow field at the tip and root of the serrations. To better understand the aerodynamic and aeroacoustic effects of serrations on the tandem configuration, the rear airfoil was equipped with several pressure taps and surface pressure transducers. Experiments were performed using a sharp sawtooth serration, for a number of tandem configurations, with different horizontal and vertical airfoil separation distances. Results have shown that a significant reduction of surface pressure fluctuation can be achieved over the leading-edge area of the rear airfoil, particularly for configurations with larger gap distance. The wake and surface pressure results have confirmed that the use of serrated trailing edges can lead to robust control of the wake flow, and reduction of wake interaction noise.

1. Introduction

The noise from rotating blades, as a component of the compressor and turbine, caused as a result of the interaction of turbulent flow from the front-blade with the rear-blade, has remained a challenging task. The reduction of blade trailing-edge noise has been investigated extensively over the past decade. To reduce trailing-edge noise, several passive methods such as serrated trailing-edge [1–12], porous surface treatments [13–16], brushes [17, 18] and morphing [19, 20] have been under investigation. Recent studies have shown that the implementation of trailing-edge serrations, such as sawtooth and slotted-sawtooth serrations, which have superior noise reduction efficiency [21], can also significantly reduce the wake turbulence intensity, particularly at high angles, where maximum aerodynamic performance is obtained [5–7]. This significant faster turbulent energy decay within the wake region is believed to be due to the three-dimensional flow originating from the serration tip and root planes. This possibility of reducing the turbulence level using serrations shows an option for a new technique for reducing noise generated by wake-airfoil interaction, such as contra-rotating propellers, rotor-stator configuration, etc.

To expand the existing knowledge and better understand the effect of using serration on the aerodynamic and acoustic performance of airfoils in tandem, detailed study of the wake development,

static pressure distributions and surface pressure fluctuations have been carried out and presented in this paper. A comprehensive aerodynamic study using a cambered NACA 65-710 airfoil with and without trailing-edge serration has been executed using the two-dimensional Particle Image Velocimetry (PIV) technique. The effect of serrations on the noise generation for the tandem NACA 65-710 configuration has also been studied by studying the surface pressure fluctuations on the rear airfoil using the remote sensing probe method. The experimental setup manufactured for the present study and the aerodynamic measurement techniques are discussed in section 2. The results and discussions are provided in section 3.

2. Experimental Setup

Experiments were carried out on tandem cambered asymmetrical NACA 65-710 airfoil in the low turbulence closed-circuit wind tunnel of the University of Bristol. The tunnel has an octagonal working section of $0.8m \times 0.6m \times 1m$, with contraction ratio of $12:1$ and capable of reaching reliable speeds of up to 100 m/s, with turbulent intensity of 0.05%. The inflow velocity used for this study is 30 m/s. The schematic of the tandem airfoils configuration with and without trailing-edge serration is shown in Fig. 1. The front and rear airfoils were manufactured from aluminium-7075 and RAKU-TOOL WB-1222 polyurethane board, respectively and machined using a computer numerical control (CNC) machine. The front airfoil was designed with a 2.3 mm blunt trailing-edge with a 15 mm depth and 0.8 mm thick slot along the span of the airfoil in order to install the flat plate (baseline) and serration inserts at the trailing-edge (see Figs. 1(a) and (c)). The rear airfoil, on the other hand, was equipped with a total number of 34 surface pressure taps on both the pressure and suction sides of the airfoil, see Figs. 1(b) and (d). The two airfoils are placed parallel to each other, in a uniform flow, and rectangular end-plates with a chamfered leading-edges were used to maintain a nearly two-dimensional flow over the two airfoils.

In the present work, the sawtooth serrations (Fig. 2(a)) were chosen based on their turbulent kinetic energy and noise reduction performance from the previous experimental studies [5–7]. The geometrical parameters of the serrations used in this study, namely the amplitude ($2h$), periodicity wavelength (λ) and the angle of serration edge (α_s), are provided in Table 1.

The wake development and the energy content study of the front airfoil with and without the trailing-edge serration were carried out using a two-component Particle Image Velocimetry (PIV). A Dantec DualPower $200mJ$ Nd:YAG laser with a wavelength of 532 nm was used to produce 1 mm thick laser sheet with the time interval between each snapshots of 23 μs and a repetition rate of 2.5 Hz. A mixture of Polyethylene glycol 80 with a mean diameter of 1 μm was used to seed the air inside the low turbulence wind tunnel. A total number of 1600 images for each measurement were captured using a FlowSense EO 4M CCD camera with a resolution of 2072 $\times$ 2072 pixels and 14 bit, corresponding to field view of 14.8 $\times$ 14.8 cm^2. The images were analysed with the DynamicStudio software from Dantec. The iterative process yield grid correlation window of 16 $\times$ 16 pixels with an overlap of 50 %, resulting in a facial vector spacing of 0.43 mm.

The geometrical parameters of the tandem airfoil configuration (Fig. 2(b)), such as the gap distances between the front and rear airfoils (W), the streamwise distance between the centre-points of the airfoils (W_x), vertical distance between the airfoils centre-points (W_y), vertical distance in the wake region (l), angle of attack of front airfoil (α_{front}) and rear airfoil (α_{rear}) are given in Table 2. Note that, W_x and W_y were defined based on the the locations where the the maximum turbulent kinetic energy is observed from the PIV results obtained for the baseline case of an isolated NACA 65-710 airfoil.

The steady and unsteady surface pressure measurements have been measured using a MicroDaq pressure scanner and remote sensing probes on both sides of the rear airfoil, see Fig. 1. The pressure taps for pressure coefficient distributions were made from 1.6 mm diameter brass tubing with 0.4 mm pinholes with the angle perpendicular to the surface of the airfoil to avoid any aerodynamic interfer-

ence between the pressure taps. The surface pressure fluctuations measurements are performed using remote sensing probes, which are connected between the brass tube to a remote microphone holder equipped with 34 Panasonic WM-61A microphones using plastic tubing with the inner and outer diameter of 0.8 mm and 3.6 mm. The data was acquired by a National Instruments PX1e-4499 at a sampling rate of 2^{16} Hz and sampling time of 8 seconds, and processed using the Matlab software.

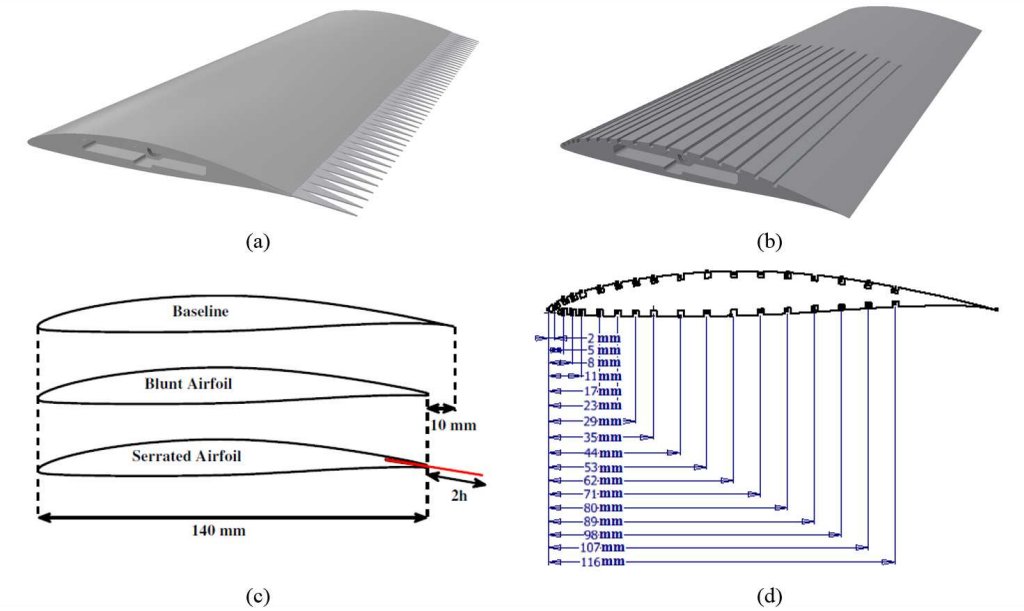

Figure 1: Tandem airfoil configuration, (a) Front airfoil model: Assembly view of NACA 65-710 with trailing-edge serration, (b) Rear airfoil model: NACA 65-710 with pressure taps distribution, (c) NACA 65-710 with and without trailing-edge serration, (d) NACA 65-710 and the locations of the pressure taps

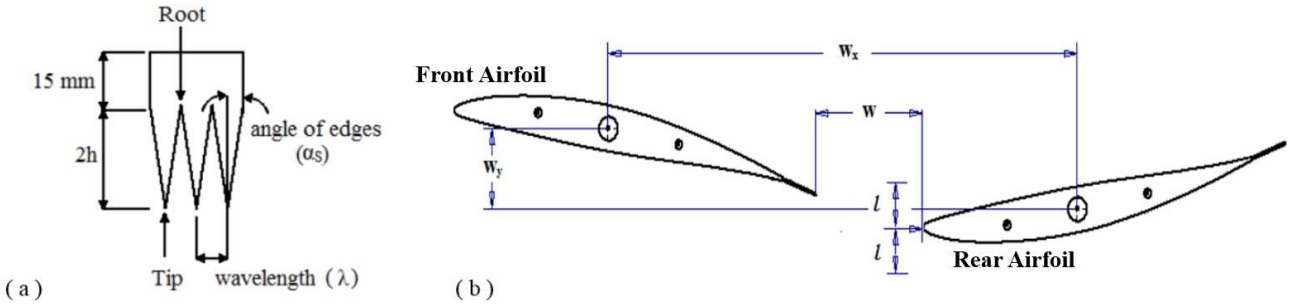

Figure 2: (a) Trailing-edge treatment: Sawtooth serration, (b) Tandem airfoil setup

Table 1: Geometrical parameters of trailing-edge treatments

Cases	Treatments	$2h$	λ	λ/h	α_s
		mm	mm		degrees
Case 1	Blunt	0	-	-	-
Case 2	Baseline	15	-	-	-
Case 3	sawtooth	30	9	0.6	8.53

Table 2: Tandem airfoil setup parameters

Cases	α_{front} degrees	α_{rear} degrees	W	W_x mm	W_y mm	$W_y + l$ mm	$W_y - l$ mm
Case 1	0	0	0.5c	299.732	17.002	-	-
Case 2	0	0	1.0c	304.732	21.502	-	-
Case 3	5	5	0.5c	229.106	25.113	-	-
Case 4	5	5	1.0c	304.106	37.113	-	-
Case 5	10	10	0.5c	227.307	30.868	35.868	25.868
Case 6	10	10	1.0c	302.307	42.368	47.368	37.368
Case 7	15	15	0.5c	224.349	-0.998	4.002	-5.998
Case 8	15	15	1.0c	299.349	2.752	7.752	-3.248

3. Results and Discussion

3.1 NACA 65-710 Airfoil Wake Measurements

To better understand the effects of serration on the wake development of the airfoil, the flow measurements of NACA 65-710 airfoil for the baseline, blunt and sawtooth serration ($\lambda = 9mm$) configurations have been carried out using Particle Image Velocimetry. The wake measurements were performed at angles of attack, AoA = 0^o, 5^o, 10^o and 15^o for the chord-based Reynolds number of $Re_c = 3 \times 10^5$, corresponding to the flow velocity of U_0 = 30 m/s. The wake profiles were captured at the downstream locations, x=0.2c to 0.8c relative to the trailing-edge of the baseline case. The wake results are only presented for the AoA = 10^o, whose results were found to show significant reduction in the turbulent kinetic energy and shear stress with the implementation of trailing-edge serration.

The wake velocity profiles and TKE results for NACA 65-710 airfoil at AoA = 10^o with and without trailing-edge serrations are presented in Figs. 3 and 4, respectively. It can be seen that the velocity profiles for sawtooth-serration has a smaller velocity deficit, especially for the root-flow case in the near-wake region (Fig. 3), x = 0.2c to 0.4c. The resultant flow after mixing for the tip- and root-flows has a similar trend compared to the baseline flow but with a significant downward deflection compared to the blunt case. A significant reduction in the turbulent kinetic energy and shear stress can be observed in Fig. 4 for both the tip- and root-flows, by up to 32 % in the near wake region, and more at the far wake locations. It can be concluded that the use of trailing-edge serration at AoA = 10^o can significantly modify the wake structure by reducing the velocity deficit in the near wake region, leading to a considerable TKE decay which is believed to be due to the interaction between the tip- and root-flow planes. The results demonstrated here are particularly important in the context of wake-interaction noise and the possibility of noise reduction in tandem airfoil configuration by stabilizing the wake flow using trailing-edge serrations. A detailed analysis will be presented in the next section for the pressure coefficient distribution and surface pressure fluctuations.

3.2 Pressure Coefficient Distribution and Surface Pressure Fluctuations

In order to quantify the effects of serrated trailing-edges on the tandem airfoil configuration, the pressure coefficient distributions and the surface pressure fluctuations of the rear NACA 65-710 airfoil for baseline and serrated (tip and root) cases have been investigated. Figure 5 presents the pressure coefficient distributions (C_p) of the rear airfoil at angles of attack, AoA = 5^o, 10^o and 15^o, with the airfoil separation distance of W = 0.5c and 1.0c. At low angle of attack, AoA = 5^o and gaps W = 0.5c and 1.0c, it can be seen that the pressure coefficient is slightly reduced on the suction side of the airfoil (upper surface) for the serrated cases (tip and root positions), while on the pressure side (lower surface), there is only a little difference between the baseline and serrated cases. Interestingly, there

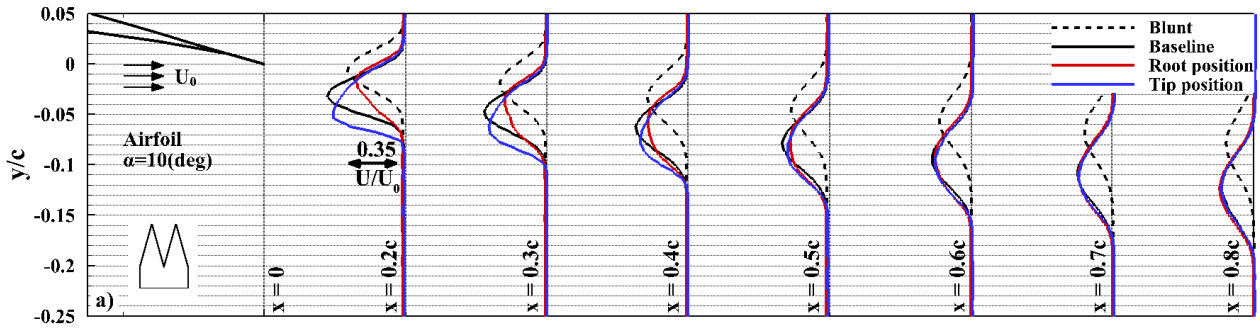

Figure 3: Wake velocity profile for serrated NACA 65-710 airfoil at AoA = 10^o and U_0 = 30 m/s. Black line: baseline; Red line: root location; Red line: tip location

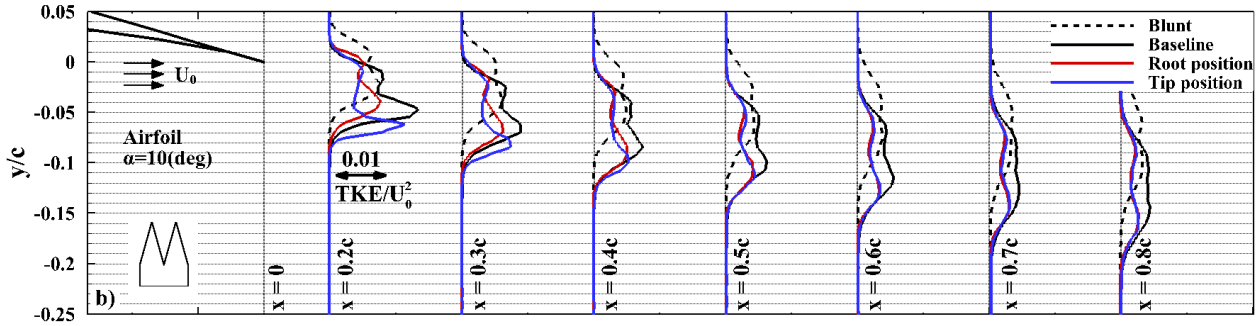

Figure 4: Wake TKE profile for serrated NACA 65-710 airfoil at AoA = 10^o and U_0 = 30 m/s. Black line: baseline; Red line: root location; Red line: tip location

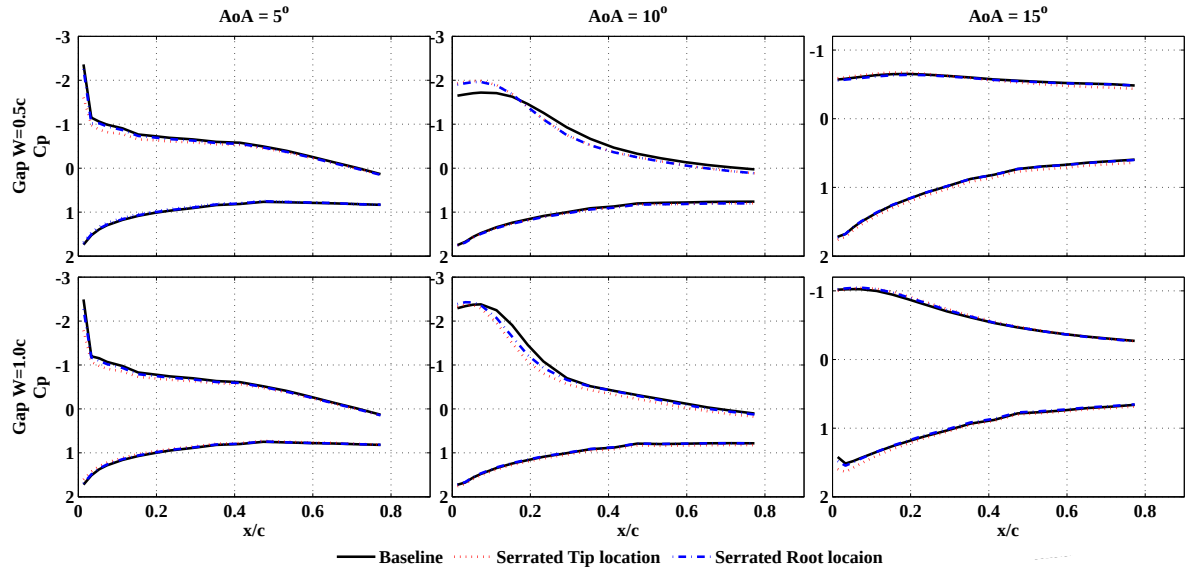

Figure 5: Pressure coefficient distribution (C_p) for baseline and serrated NACA 65-710 airfoils at AoA = 5^o, 10^o, 15^o, at U_0 = 30 m/s with airfoil separation distance of W = $0.5c$ and $1.0c$.

is a significant change in the C_p distribution at the airfoil suction side for AoA = 10^o. At AoA = 10^o, with $W = 0.5c$, the C_p increases in the near leading-edge region ($x/c < 0.15$) and reduces significantly at downstream of the leading-edge over the airfoil suction side. Comparison of the gaps between the tandem airfoils show that the larger gap ($W = 1.0c$), at AoA = 10^o on the suction side has a small increase in the near leading-edge ($x/c < 0.1$), but a significant reduction in the region up to $0.3c$. Nonetheless, the results obtained for the pressure side of the airfoil ($W = 0.5c$ and $1.0c$) remained similar for both the baseline and serrated cases. At higher angles of attack, AoA = 15^o, $W = 0.5c$, only a mild change in C_p can be observed on both the suction and pressure sides of the airfoil for the serrated cases. However, at $W = 1.0c$, the C_p at the airfoil suction side shows an increase for the serrated cases over half of the chord distance whereas over the pressure side, the C_p drops a little, especially in the near leading-edge locations. Note that, pronounced changes of C_p in the serrated cases can be seen at higher angles of attack, especially at AoA = 10^o. The changes observed are likely to be due to the lower wake-turbulent interaction between the tandem airfoils, which is in agreement with the results obtained in Fig. 4, where the serrated case has noticeably reduced the turbulent kinetic energy downstream of the front airfoil.

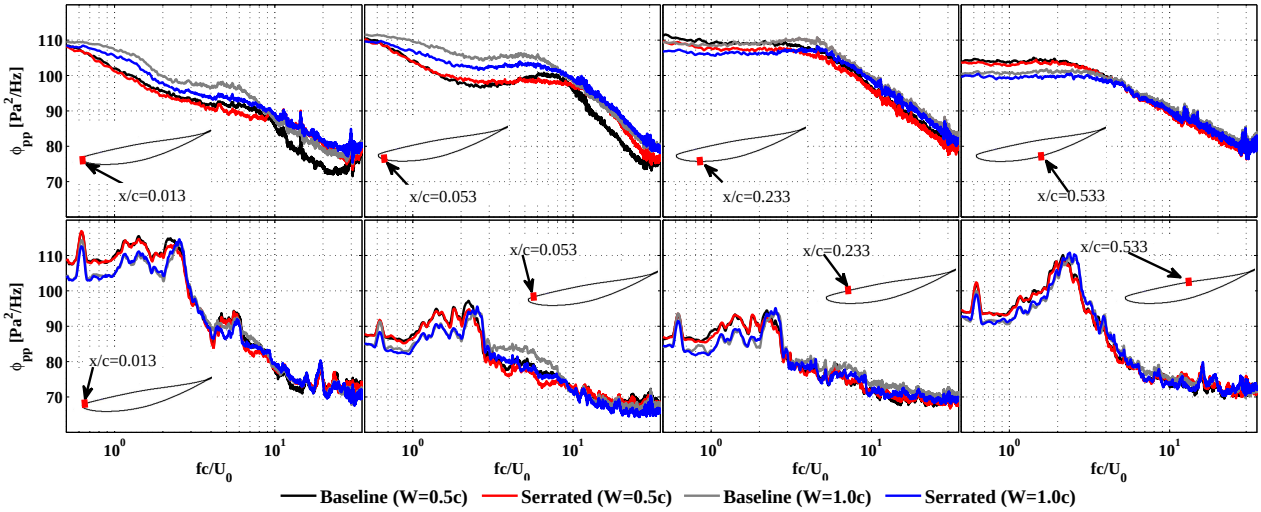

Figure 6: Surface pressure fluctuations results for baseline and serrated NACA 65-710 airfoils at AoA = 10^o, W = $0.5c$ and $1.0c$ at U_0 = 30 m/s.

In order to further demonstrate the effectiveness of serration treatments for reducing aerodynamic loading and noise, surface pressure fluctuation measurements on the rear airfoil have been conducted using the remote sensing probe method. The results are presented for the AoA = 10^o, based on the results seen in Figs. 4 and 5. Figure 6 presents the surface pressure fluctuations (ϕ_{pp}) results for the baseline and serrated tandem airfoils at AoA = 10^o, W=0.5c and 1.0c at x/c = 0.013, 0.053, 0.233 and 0.533 for both the suction (upper row) and pressure (bottom row) sides of the rear airfoil. At $W = 0.5c$, the intensity of pressure fluctuations in the near leading-edge region (x/c = 0.013) for the serrated case is reduced clearly in the low fc/U_0 region, but a significant increase of ϕ_{pp} can be seen at $fc/U_0 > 9$. At x/c = 0.053, the ϕ_{pp} changes in the entire fc/U_0 region for the serrated case, where the pressure fluctuations increases at the fc/U_0 range between 1.5 to 4.0, decreases in the mid-fc/U_0 region and increase significantly at $fc/U_0 > 10$. However, at x/c = 0.233 and 0.533, the ϕ_{pp} of the serrated case reduces moderately in the low fc/U_0 region and became almost similar to that of baseline case at higher fc/U_0 region ($fc/U_0 > 4.0$). It can also be seen that the pressure fluctuations of the serrated cases on the suction side with $W = 1.0c$ for all the measured locations (x/c = 0.013, 0.053, 0.233, 0.533) are relatively low for $fc/U_0 < 10$, while almost no changes in ϕ_{pp} is seen between the serrated and baseline case at $fc/U_0 > 10$. Also, the intensity of pressure fluctuations on the pressure

side at all the measurement locations for both the baseline and serrated cases (W = 0.5c and 1.0c) are observed to be similar for the entire fc/U_0 range, but noticeable reductions of the ϕ_{pp} broadband spectral amplitude is seen on the pressure side (x/c = 0.053, 0.233), at downstream locations from the leading-edge of the rear airfoil.

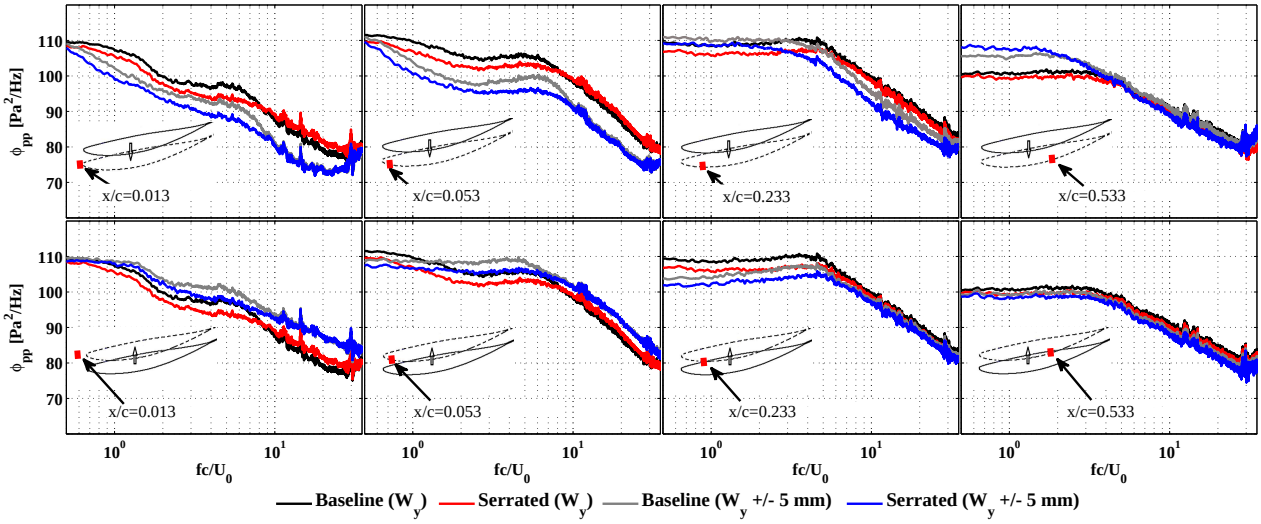

Figure 7: Surface pressure fluctuations result for serrated and unserrated NACA 65-710 airfoil at AoA = 10^o, W = 1.0c with vertical distance of l = 5 mm at U_0 = 30 m/s.

Figure 7 shows the ϕ_{pp} results for the suction side of the baseline and serrated cases at AoA = 10^o, W = 1.0c, at different vertical distances (l = $\pm$5 mm) between the tandem airfoils, respective to the original position of the airfoils. The positive and negative values of l refers to upward and downward location of the airfoil, relative to its origin position (see Fig 2(b)). As the rear airfoil moved 5 mm downwards relative to the original location, clear reduction in ϕ_{pp} for all the serrated cases can be observed at the near leading-edge locations (x/c = 0.013 and 0.053) over the fc/U_0 region of up to 8.0 and became similar to that of baseline case at (fc/U_0 > 8.0). At x/c = 0.233, a consistent reduction in ϕ_{pp} can be seen for the serrated case over the entire range of fc/U_0. Moreover, at further downstream locations of the rear airfoil, a significant increase in the ϕ_{pp} amplitude can be seen for the l=-5 mm case, compared to its original location and it is also noticed that the ϕ_{pp} of the serrated case increases in the low fc/U_0 region, and both the cases are almost identical at the high fc/U_0 region. Results also have shown that, moving the rear airfoil 5 mm upwards can lead to the reduction of ϕ_{pp} in the low and mid-fc/U_0 region for the serrated case. At x/c=0.533, it is noted that the ϕ_{pp} obtained for the baseline and serrated cases for the two positions (l = +5 mm and 0 (original position)) were almost similar especially in the higher fc/U_0 region. As shown in the results obtained from Figs. 4 and 5, it can be concluded that the use of serrations leads to significant reduction of the surface pressure fluctuations especially at low frequencies in the near leading-edge locations of the rear airfoil. This is believed to be due to the significant reduction in the energy content of the turbulent-wake flow structures within the gap.

4. Conclusion

An extensive experimental study has been carried out using serration treatments as a means to control the wake development and hence the noise generation from tandem airfoils. The flow analysis have shown that the energy content of the wake flow can be reduced by fitting the front airfoil with serrated trailing-edge. This is particularly obvious at high angles of attack. The surface pressure fluctuation results over the leading edge of the rear airfoil have also shown that the use of trailing-

edge serration on the front airfoil can lead to significant reduction of surface pressure fluctuations on the rear airfoil. The reduction of unsteady aerodynamic loading on the rear airfoil can be interpreted as potential control of the noise generation mechanism. Further experiments, including far-field noise measurements are planned to better understand the effect of trailing-edge serrations in the context of tandem airfoil configurations.

References

1. Sandberg, R. and Jones, L. Direct numerical simulations of low reynolds number flow over airfoils with trailing-edge serrations, *Journal of Sound and Vibration*, **330** (16), 3818–3831, (2011).
2. Moreau, D., Brooks, L. and Doolan, C. On the noise reduction mechanism of a flat plate serrated trailing edge at low-to-moderate reynolds number, *18th AIAA/CEAS aeroacoustics conference (33rd AIAA aeroacoustics conference)*, (AIAA 2012-2186).
3. Chong, T., Joseph, P. and Gruber, M. Airfoil self noise reduction by non-flat plate type trailing edge serrations, *Applied Acoustics*, **74** (4), 607–613, (2013).
4. Ji, L., Qiao, W., Tong, F., Xu, K. and Chen, W. Experimental and numerical study on noise reduction mechanisms of the airfoil with serrated trailing edge, *20th AIAA/CEAS Aeroacoustics Conference*, (AIAA 2014-3297).
5. Liu, X., Azarpeyvand, M. and Theunissen, R. Aerodynamic and aeroacoustic performance of serrated airfoils, *21st AIAA/CEAS Aeroacoustics Conference*, (AIAA 2015-2201).
6. Liu, X., Azarpeyvand, M. and Theunissen, R. On the aerodynamic performance of serrated airfoils, *22nd International Congress on Sound and Vibration*, pp. 12–16, (2015).
7. Liu, X., Kamliya Jawahar, H., Azarpeyvand, M. and Theunissen, R. Wake development of airfoils with serrated trailing edges, *22nd AIAA/CEAS Aeroacoustics Conference*, (AIAA 2016-2817).
8. Avallone, F., Arce Leon, C., Pröbsting, S., Lynch, K. P. and Ragni, D. Tomographic-PIV investigation of the flow over serrated trailing-edges, *54th AIAA Aerospace Sciences Meeting*, (AIAA 2016-1012).
9. Chong, T. P. and Joseph, P. F. An experimental study of airfoil instability tonal noise with trailing edge serrations, *Journal of Sound and Vibration*, **332** (24), 6335–6358, (2013).
10. Azarpeyvand, M., Gruber, M. and Joseph, P. An analytical investigation of trailing edge noise reduction using novel serrations, *19th AIAA/CEAS aeroacoustics conference*, (AIAA 2013-2009).
11. Gruber, M., Azarpeyvand, M. and Joseph, P. F. Airfoil trailing edge noise reduction by the introduction of sawtooth and slitted trailing edge geometries, *20th International Congress on Acoustics*, **10**, 6, (2010).
12. Gruber, M., Joseph, P. and Azarpeyvand, M. An experimental investigation of novel trailing edge geometries on airfoil trailing edge noise reduction, *19th AIAA/CEAS Aeroacoustics Conference*, (A1AA 2013-2011).
13. Vathylakis, A., Chong, T. P. and Joseph, P. F. Poro-serrated trailing-edge devices for airfoil self-noise reduction, *AIAA Journal*, **53** (11), 3379–3394, (2015).
14. Showkat Ali, S. A., Szoke, M., Azarpeyvand, M. and Ilário, C. Trailing edge bluntness flow and noise control using porous treatments, *22nd AIAA/CEAS Aeroacoustics Conference*, (AIAA 2016-2832).
15. Showkat Ali, S. A., Liu, X. and Azarpeyvand, M. Bluff body flow and noise control using porous media, *22nd AIAA/CEAS Aeroacoustics Conference*, (AIAA 2016-2754).
16. Showkat Ali, S. A., Azarpeyvand, M., da Silva and Ilário, C. Boundary layer interaction with porous surface and implications for aerodynamic noise, *23rd International Congress on Sound & Vibration*, (ICSV 2016).
17. Herr, M. and Dobrzynski, W. Experimental investigations in low-noise trailing edge design., *AIAA journal*, **43** (6), 1167–1175, (2005).
18. Finez, A., Jacob, M., Jondeau, E. and Roger, M. Broadband noise reduction with trailing edge brushes, *16th AIAA/CEAS Aeroacoustics Conference*, (AIAA 2010-3980).
19. Ai, Q., Azarpeyvand, M., Lachenal, X. and Weaver, P. M. Aerodynamic and aeroacoustic performance of airfoils with morphing structures, *Wind Energy*, (Vol. 19, No. 7, 2016, pp. 1325-1339).
20. Ai, Q., Azarpeyvand, M., Lachenal, X. and Weaver, P. M. Airfoil noise reduction using morphing trailing edge, *21st International Congress on Sound and Vibration*, (2014).
21. Gruber, M. Airfoil noise reduction by edge treatments, *Thesis, University of Southampton*, (2012).